Seismic Velocities in Dry and Saturated Cracked Solids

RICHARD J. O'CONNELL

Department of Geological Sciences and Center for Earth and Planetary Physics
Harvard University, Cambridge, Massachusetts 02138

BERNARD BUDIANSKY

Division of Engineering and Applied Physics and Center for Earth and Planetary Physics
Harvard University, Cambridge, Massachusetts 02138

The elastic moduli of a solid permeated with an isotropic distribution of flat cracks have been calculated from the energy of a single crack by use of a self-consistent approximation. The results are applicable for a dense network of cracks and give physically reasonable results up to the point that the shear modulus vanishes. Results for both circular and elliptical cracks are essentially the same if the crack density is characterized by $2N\langle A^2/P\rangle/\pi$, where N is the number of cracks per unit volume, A is the area of crack, and P is the perimeter of cracks; for circular cracks of radius a this becomes $N\langle a^3\rangle$. This crack density parameter can be related quantitatively to crack traces observed in thin section. Results for completely dry or saturated cracks, for mixtures of dry and saturated cracks, and for cracks saturated with a compressible fluid are presented. For all cases, both seismic wave velocities decrease with increasing crack density. The velocity ratio V_P/V_S decreases for dry cracks and increases for saturated cracks. For the analysis of data a plot of V_P/V_S versus V_S uniquely specifies the crack density. Comparison of the theory with wave velocities measured in laboratory rock samples demonstrates its validity for large crack densities. Interpretation of velocity changes before the San Fernando earthquake indicates that the region contained a substantial density of cracks at all times, that the anomalous decrease in V_P/V_S was due to the vaporization of pore fluid in nearly all of the previously saturated cracks without the introduction of new dry cracks, and that during the period of the recovery of the velocities to previous values the number of cracks in the region away from the epicentral zone decreased as they were resaturated, whereas the crack density increased following resaturation in the epicentral zone. Such use of the theoretical results may be useful in further investigations of preseismic phenomena.

The influence of internal cracks and pores on the elastic properties of rocks has been recognized for some time and has received considerable attention in the literature. The effects are most apparent in laboratory measurements of some elastic properties of a rock sample as a function of hydrostatic pressure, usually over a range of several kilobars. If the sample is covered with an impermeable jacket, the modulus measured (e.g., bulk modulus, Young's modulus, or elastic wave velocity) usually increases markedly with increasing pressure. This effect is generally interpreted as being due to the fact that the cracks are squeezed closed by the external pressure until ultimately they no longer have an appreciable effect on the elastic properties of the rock. This effect was first noticed and interpreted in this way by *Adams and Williamson* [1923] and has been noted and similarly interpreted by subsequent workers. *Birch* [1960, 1961] presents measurements of the compressional wave velocities for a large number of rocks that exhibit this effect and discusses the effects of cracks and porosity, summarizing previous work.

That the effect is due primarily to the closing of cracks and not spherelike pores is evidenced by the low porosities (<1%) of many of the samples and the relatively low pressures required to raise the moduli to values near those expected for a rock free of cracks. As *Walsh* [1965*a*] pointed out, a few kilobars are enough to close cracks having aperture to diameter aspect ratios of the order of 10^{-3}. Such cracks are also consistent with the assumed nature of porosity in holocrystalline igneous rocks arising from cracks or minute openings along grain boundaries, which could have opened from changes in temperature or pressure altering the shape of anisotropic mineral grains [*Birch*, 1961; *Spetzler et al.*, 1972], so that they no longer fit together without openings between them. Whether such cracks are a common feature of rocks in place in the crust is not clear at present [*Simmons and Nur*, 1968], although there are suggestions from detailed observations of cracks [*Brace et al.*, 1973] that such indeed may be the case. On a larger scale, joints and macroscopic fractures could also constitute flat cracks.

Earlier theoretical analyses of the effect of cracks on the elastic properties of solids have been intended to apply only to dilute concentrations of cracks, in which the cracks are presumed to be sufficiently far apart to permit the independent evaluation of the effect of each crack on the properties of the uncracked material. *Walsh* [1969] in a study that improved and extended his earlier work [1965*a*, *b*, 1968] calculated the influence of both dry and saturated cracks on this basis. He assumed that the cracks were nearly flat oblate spheroids, and his results were based on *Wu*'s [1966] paper on the influence of general ellipsoidal inclusions on elastic properties. (Wu's work, in turn, was directly based on the now classic paper of *Eshelby* [1957].) *Garbin and Knopoff* [1973] made an independent analysis for the limiting case $c/a \to 0$ (c = minor semiaxis and a = major semiaxis of the spheroid), obtaining results in agreement with those of *Walsh* [1969] for the reduction in the P wave velocity due to a dilute crack distribution.

The present paper summarizes the results of a study [*Budiansky and O'Connell*, 1974] in which very thin randomly oriented ellipsoidal cracks (with semiaxes $a > b \gg c$) are treated in a self-consistent fashion that hopefully provides a reasonable estimate for macroscopic properties even when many closely spaced cracks are present. Both dry and saturated cracks are considered. Attention is also directed to

the possibilities of partial saturation and to saturation with anomalously compliant fluids (e.g., high-pressure steam). Predictions of the theory are compared with the data of *Nur and Simmons* [1969], who systematically measured velocities in a number of rocks, both dry and saturated, as a function of pressure. It is shown how a sequence of measurements of elastic wave velocities may be used in conjunction with the theory to infer the corresponding history of crack concentration and saturation. Finally, such inferences are drawn for both the epicentral region and an adjacent region of the 1971 San Fernando earthquake.

MODULI OF CRACKED SOLIDS

Dry circular cracks. A very brief outline of the self-consistent energy approach used to analyze cracked bodies [*Budiansky and O'Connell,* 1974] will be given together with the main results. Let Φ be the isothermal potential energy (strain energy plus load potential) of the uncracked body under a prescribed loading and let $\bar{\Phi}$ be the corresponding quantity for the cracked body. Then

$$\bar{\Phi} = \Phi + \Delta\Phi \tag{1}$$

where $\Delta\Phi$ is the potential energy change due to insertion of cracks. The approximate calculation of effective elastic constants of the cracked body is achieved by means of plausible estimates for $\Delta\Phi$ for various loading conditions. Thus under a pure hydrostatic stress s, $\Phi = -(s^2V/2K)$, where V is the volume and K the bulk modulus of the material. In a sufficiently large volume of material with randomly oriented cracks an effective bulk modulus $\bar{K}$ provides the potential energy $\bar{\Phi} = -(s^2V/2\bar{K})$. Now consider flat spheroidal cracks ($a = b >> c$) and estimate $\Delta\Phi$ by assuming that each crack contributes to $\Delta\Phi$ as if it were an isolated crack in an infinite matrix having the as yet unknown properties of the cracked body. For the limiting case of $c/a \to 0$ this gives an energy loss for each crack denoted by

$$\frac{8a^3s^2}{9\bar{K}}\left(\frac{1-\bar{\nu}^2}{1-2\bar{\nu}}\right) \tag{2}$$

where $\bar{\nu}$ is the effective Poisson ratio of the cracked body. Accordingly, from (1),

$$-\frac{s^2V}{2\bar{K}} = -\frac{s^2V}{2K} - \frac{8s^2}{9\bar{K}}\frac{1-\bar{\nu}^2}{1-2\bar{\nu}}\sum a^3 \tag{3}$$

where the summation is over all cracks. Hence with N cracks per unit volume and the crack density parameter defined by

$$\epsilon \equiv \frac{1}{V}\sum a^3 \equiv N\langle a^3\rangle \tag{4}$$

we obtain

$$\frac{\bar{K}}{K} = 1 - \frac{16}{9}\left(\frac{1-\bar{\nu}^2}{1-2\bar{\nu}}\right)\epsilon \tag{5}$$

Analogous derivations provide the results for the effective Young modulus $\bar{E}$ and shear modulus $\bar{G}$:

$$\frac{\bar{E}}{E} = 1 - \frac{16}{45}\frac{(1-\bar{\nu}^2)(10-3\bar{\nu})}{(2-\bar{\nu})}\epsilon \tag{6}$$

$$\frac{\bar{G}}{G} = 1 - \frac{32}{45}\frac{(1-\bar{\nu})(5-\bar{\nu})}{(2-\bar{\nu})}\epsilon \tag{7}$$

The effective Poisson ratio $\bar{\nu}$ is related to ϵ and ν of the uncracked solid by

$$\epsilon = \frac{45}{16}\frac{(\nu-\bar{\nu})(2-\bar{\nu})}{(1-\bar{\nu}^2)(10\nu-3\nu\bar{\nu}-\bar{\nu})} \tag{8}$$

To calculate the effective moduli for a given ϵ, (8) must first be solved for $\bar{\nu}$, after which (5)–(7) can be evaluated directly.

Had the self-consistent approximation not been made, (2) would contain K and ν instead of $\bar{K}$ and $\bar{\nu}$. This change results in

$$\frac{\bar{K}}{K} = \left[1 + \frac{16}{9}\left(\frac{1-\nu^2}{1-2\nu}\right)\epsilon\right]^{-1}$$

an explicit result that agrees with (5) only for sufficiently small ϵ. Similar non-self-consistent results can be obtained for $\bar{G}$ and $\bar{E}$; their relation to (6) and (7) is exactly analogous to the relation between (5) and the non-self-consistent result for $\bar{K}$.

The effective moduli as a function of crack density are shown in Figure 1 for three values of ν, the Poisson ratio of the uncracked solid. All the moduli approach zero uniformly as ϵ increases and vanish exactly for $\epsilon = 9/16$. The accuracy of the self-consistent results for ϵ near 9/16 is not known; surely, the statistics of the crack distribution and intersections of cracks eventually invalidate the approximation. Nevertheless, the solid should become noncoherent for some finite value of ϵ, and the self-consistent results indicate that trend. It may be of interest to note that in the analogous problem of the electrical conductivity of a three-dimensional array of resistors where a certain number of the resistors are removed at random, a self-consistent calculation gives results that are reliable up to an 80–90% reduction in conductivity [*Shankland and Waff,* 1974; *Kirkpatrick,* 1973]. This suggests that the elastic solution may be quite accurate to a crack density of $\epsilon = 0.4$ or more. This corresponds to one crack of radius 3/4 per unit volume.

The effect on $\bar{E}/E$ and $\bar{G}/G$ of varying Poisson's ratio of the matrix is small. The nearly linear dependence of $\bar{\nu}$ on ϵ indicates that the solution of (8) may be well approximated by

$$\bar{\nu} = \nu\left(1 - \frac{16}{9}\epsilon\right)$$

which simplifies the calculation of the effective moduli in (5)–(7) considerably.

Dry elliptical cracks. For general flat elliptical cracks ($a \geq b$, $c/a \to 0$) a similar derivation gives the same result for $\bar{K}/K$ as that for circular cracks, (5), the crack density parameter ϵ being redefined as

$$\epsilon = (2N/\pi)\langle A^2/P\rangle \tag{9}$$

where A is the area of a crack πab and P is the perimeter given by $4aE(k)$, where $E(k)$ is a complete elliptic integral defined in the appendix. For circular cracks ($a = b$) the more general definition (9) reduces to (4).

Unlike the result for $\bar{K}$ the results for $\bar{E}$ and $\bar{G}$ depend explicitly on the ellipticity of the cracks through the ratio b/a and are given by

$$\frac{\bar{E}}{E} = 1 - \frac{16}{45}(1-\bar{\nu}^2)[3 + T(b/a, \bar{\nu})]\epsilon \tag{10}$$

$$\frac{\bar{G}}{G} = 1 - \frac{32}{45}(1-\bar{\nu})[1 + \tfrac{3}{4}T(b/a, \bar{\nu})]\epsilon \tag{11}$$

where $T(b/a, \bar{\nu})$ is a messy expression including elliptic integrals given in the appendix. The equation for Poisson's ratio becomes

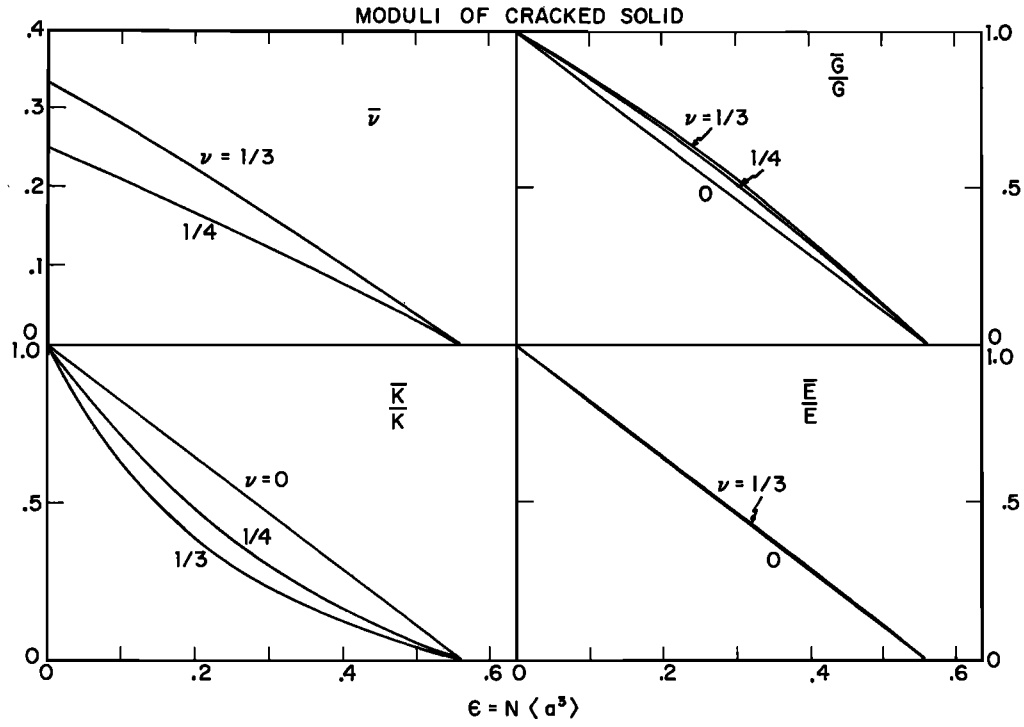

Fig. 1. Poisson's ratio $\bar{\nu}$, the effective bulk modulus $\bar{K}$, shear modulus $\bar{G}$, and Young's modulus $\bar{E}$ for a solid permeated with N dry circular cracks of radius a per unit volume. The moduli are normalized to the values K, G, and E for an uncracked solid. Results are shown for three values of Poisson's ratio ν for the uncracked solid: $\nu = 0$, 1/4, and 1/3. For the case $\nu = 0$ the effective Poisson's ratio $\bar{\nu} = 0$ for all ϵ.

$$\epsilon = \frac{45}{8} \frac{(\nu - \bar{\nu})}{(1 - \bar{\nu}^2)[2 - T + 2\nu(3 + T)]} \tag{12}$$

For circles ($b = a$), $T = 4/(2 - \bar{\nu})$, and the results above reduce to those for circular cracks. We note, however, that $T(b/a, 0) = 2$ for all values of b/a and that the limiting value of ϵ remains 9/16 for all values of b/a. In fact, the final numerical results for elliptical cracks are indistinguishable for all ϵ from those for circular cracks, as is shown in Figure 1. The results for circular cracks (equations (5)–(8)) may therefore be used for the more general case with negligible error. Indeed the near coincidence of the results for circular and elliptical cracks suggests that the effects of cracks of any convex shape would be similar to those for circular cracks as long as their density is characterized by the same parameter ϵ defined in (9) in terms of area and perimeter.

This characterization of crack density indicates that large cracks reduce the moduli more than a greater number of small cracks with the same total crack area. Thus if small cracks coalesce into a smaller number of larger cracks (e.g., by small extensions of the small cracks), the result would be a substantial increase in the crack density parameter and a corresponding reduction of the elastic moduli of the solid.

Saturated elliptical cracks. Suppose that each crack is filled with a fluid of bulk modulus $\bar{K}$. The calculation of $\Delta\Phi$ in the energy balance (1) must now take into account the elastic energy of the fluid as well as the effect of its presence on the elastic state of the surrounding material. Execution of this calculation in the limit $c/a \to 0$, $\bar{K} \neq 0$ shows that in this limiting case the effect of the fluid is to 'glue' the opposing faces of the crack together with respect to relative normal displacement of the faces while not inhibiting relative sliding of the crack faces. This leads directly to the results

$$\frac{\bar{K}}{K} = 1$$

$$\frac{\bar{E}}{E} = 1 - \frac{16}{45}(1 - \bar{\nu}^2)T\epsilon \tag{13}$$

$$\frac{\bar{G}}{G} = 1 - \frac{8}{15}(1 - \bar{\nu})T\epsilon$$

for saturated elliptical cracks. The equation for Poisson's ratio is

$$\epsilon = \frac{45}{8} \frac{(\bar{\nu} - \nu)}{(1 - \bar{\nu}^2)(1 - 2\nu)T} \tag{14}$$

For the special case $\nu = 1/4$ the results of (13) and (14) are shown in Figure 2 for the two extreme cases $b/a = 0$ and $b/a = 1$, together with the results (equations (5) and (10)–(12)) for dry elliptical cracks for comparison. For circular cracks ($b/a = 1$ and $T = 4/(2 - \bar{\nu})$) the limiting value of ϵ is now 45/32 instead of 9/16 as it was for dry cracks. Furthermore, $\bar{\nu}$ increases with ϵ, approaching 1/2 as the limiting value of ϵ is approached. For very long slender saturated cracks ($b/a \to 0$) the limiting value of ϵ is 5/4, slightly less than the value for circular cracks. Nevertheless, the results for the moduli as functions of ϵ for the two limiting cases $b/a = 0$, 1 are sufficiently close to one another to permit the use of the circular crack results as good approximations for those for cracks of any ellipticity.

The large difference between the limiting values of ϵ for the dry and saturated cases may indicate the limitations inherent in the self-consistent approach for very large crack densities. Nevertheless, the trends predicted may be reliable, and the appropriate interpretation of the theory in the vicinity of the critical crack concentration is that the elastic stiffnesses of the

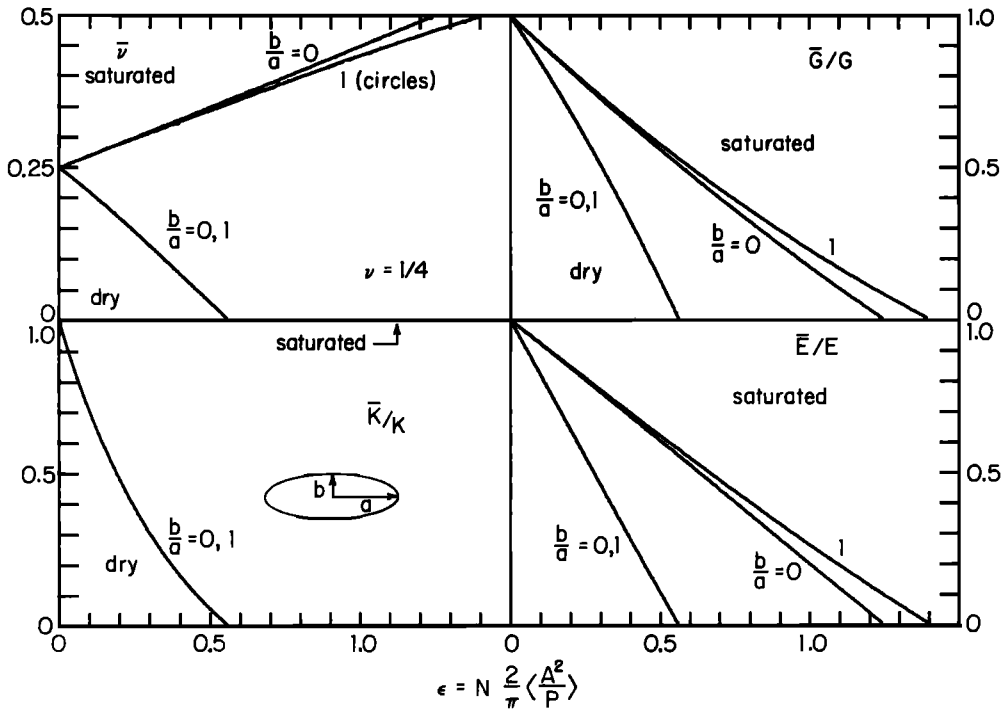

Fig. 2. Poisson's ratio, effective bulk modulus $\bar{K}$, shear modulus $\bar{G}$, and Young's modulus $\bar{E}$ of a solid with either dry or saturated elliptical cracks. Results are shown for circular cracks (b/a = 1) and for the limiting case of extremely elliptical cracks (b/a = 0). For dry cracks the two cases are indistinguishable, and for saturated cracks the difference is small. The crack density is $\epsilon = 2N\langle A^2/P\rangle/\pi$, where A is the area and P the perimeter of a crack; this reduces to $\epsilon = N\langle a^3\rangle$ for circular cracks.

material are very likely to have been reduced to extremely small fractions of the values for an uncracked solid.

Saturated circular cracks. For easy reference the results for circular cracks, obtained by substituting $T = 4/(2 - \bar{\nu})$ in (13) and (14) are

$$\frac{\bar{K}}{K} = 1$$

$$\frac{\bar{E}}{E} = 1 - \frac{64}{45}\left(\frac{1 - \bar{\nu}^2}{2 - \bar{\nu}}\right)\epsilon \qquad (15)$$

$$\frac{\bar{G}}{G} = 1 - \frac{32}{15}\left(\frac{1 - \bar{\nu}}{2 - \bar{\nu}}\right)\epsilon$$

$$\epsilon = \frac{45}{32}\frac{(\bar{\nu} - \nu)(2 - \bar{\nu})}{(1 - \bar{\nu}^2)(1 - 2\nu)} \qquad (16)$$

In the remainder of this paper, only results for circular cracks will be used with the understanding that the definition (9) for ϵ rather than (4) will render them applicable with little error to elliptical cracks and probably to cracks of any convex shape as well.

Partial saturation. Suppose that N_1 of the cracks per unit volume are dry and that $N_2 = N - N_1$ are saturated. It is easy to show then that in terms of the saturated fraction $\xi = N_2/N$ the results for the moduli of a body containing a random distribution of partially saturated circular cracks are

$$\frac{\bar{K}}{K} = 1 - \frac{16}{9}\left(\frac{1 - \bar{\nu}^2}{1 - 2\bar{\nu}}\right)(1 - \xi)\epsilon$$

$$\frac{\bar{E}}{E} = 1 - \frac{16}{45}(1 - \bar{\nu}^2)\left[3(1 - \xi) + \frac{4}{2 - \bar{\nu}}\right]\epsilon \qquad (17)$$

$$\frac{\bar{G}}{G} = 1 - \frac{32}{45}(1 - \bar{\nu})\left[1 - \xi + \frac{3}{2 - \bar{\nu}}\right]\epsilon$$

and the equation for $\bar{\nu}$ is

$$\epsilon = \frac{45}{16}\left(\frac{\nu - \bar{\nu}}{1 - \bar{\nu}^2}\right)\cdot\frac{(2 - \bar{\nu})}{[(1 - \xi)(1 + 3\nu)(2 - \bar{\nu}) - 2(1 - 2\nu)]} \qquad (18)$$

Numerical results (for ν = 1/4) are shown in Figure 3 for various values of ξ. The end points of the $\bar{\nu} - \epsilon$ curves lie along

$$\epsilon = \frac{9}{32}\frac{(1 + 3\bar{\nu})(2 - \bar{\nu})}{(1 - \bar{\nu}^2)} \qquad (19)$$

and the limiting values of $\bar{\nu}$ are in turn related to ξ by

$$\xi = 1 - \frac{2(1 - 2\bar{\nu})}{(2 - \bar{\nu})(1 + 3\bar{\nu})} \qquad (20)$$

These results for partial saturation also apply to situations in which some of the cracks are only partly filled with liquid, the rest of the crack space containing a high-compressibility vapor phase. Such cracks should be considered dry as far as their effect on elastic properties is concerned.

Soft-fluid saturation. The limiting results for saturated circular cracks given above for $c/a \to 0$ can be inadequate for very small c/a if the bulk modulus of the fluid $\bar{K}$ is in a range intermediate to very low and moderately high values. In the analysis the parameter

$$\omega = \frac{a}{c}\frac{\bar{K}}{K} \qquad (21)$$

turns out to be crucial, and it is useful to consider the limiting mathematical values of the effective moduli for $c/a \to 0$ but to keep ω fixed and equal to its actual value for $\bar{K}/K \neq 0$ and $c/a \neq 0$. Then $\omega = 0$ corresponds to the case of dry cracks, and $\omega = \infty$ to the saturated case. With $\bar{K}/K \sim 10^{-6}$, as would be the

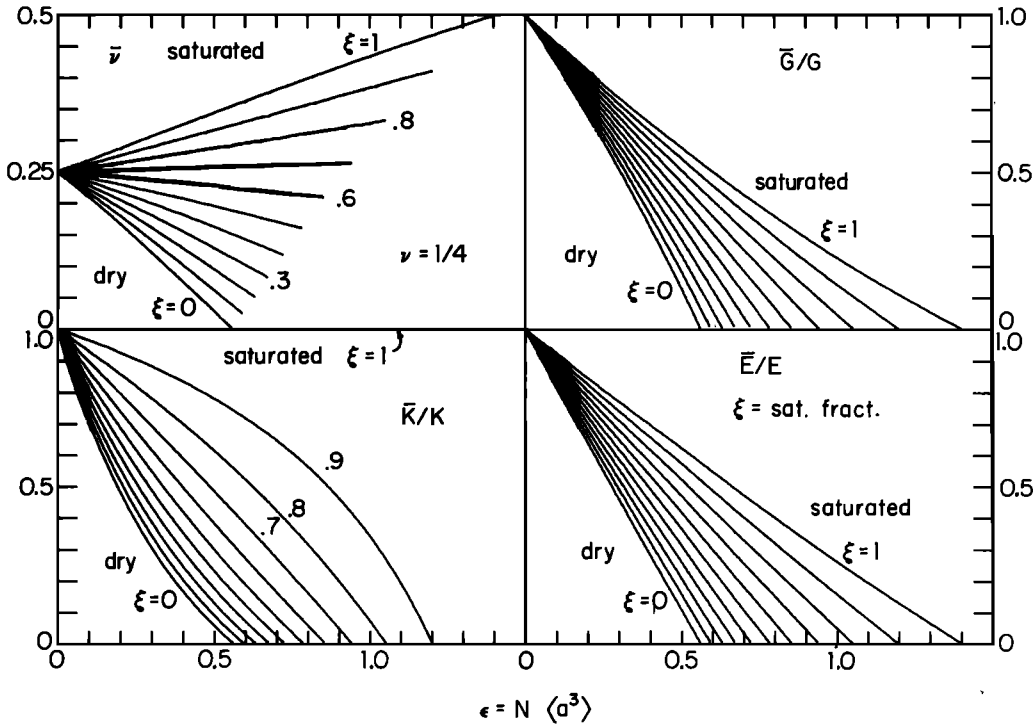

Fig. 3. Effective elastic properties of a solid with N circular cracks per unit volume, a fraction ξ of which are saturated with a fluid and the remainder are empty. The results for completely dry cracks ($\xi = 0$) are identical to those in Figure 1 for $\nu = 1/4$; the results for completely saturated cracks are identical to those in Figure 2 for $b/a = 1$.

case for air-filled cracks in rock, and $c/a \sim 10^{-3}$, ω is indeed very small. On the other hand, for water-saturated cracks, $\bar{K}/K \sim 3 \times 10^{-2}$, giving $\omega \sim 30$, and this, as we shall see, gives results near those for $\omega = \infty$, justifying the use of the saturated crack results for this case. However, *Anderson and Whitcomb* [1973] have pointed out that water at midcrustal depths and temperatures has properties such that $\bar{K}/K \sim 10^{-3}$, giving $\omega \sim 1$, so that neither of the extreme situations that we have so far contemplated would be applicable. Fortunately, this intermediate case is also amenable to straightforward solution. In terms of the parameter ω (assumed to be the same for all cracks) the appropriate equations are [*Budiansky and O'Connell*, 1974]

$$\frac{\bar{K}}{K} = 1 - \frac{16}{9}\frac{(1-\bar{\nu}^2)}{(1-2\bar{\nu})} D\epsilon$$

$$\frac{\bar{E}}{E} = 1 - \frac{16}{45}(1-\bar{\nu}^2)\left[3D + \frac{4}{(2-\bar{\nu})}\right]\epsilon \qquad (22)$$

$$\frac{\bar{G}}{G} = 1 - \frac{32}{45}(1-\bar{\nu})\left[D + \frac{3}{(2-\bar{\nu})}\right]\epsilon$$

$$\epsilon = \frac{45}{16}\frac{(\nu-\bar{\nu})}{(1-\bar{\nu}^2)}\frac{(2-\bar{\nu})}{[D(1+3\nu)(2-\bar{\nu}) - 2(1-2\nu)]} \qquad (23)$$

$$D = \left[1 + \frac{4}{3\pi}\frac{(1-\bar{\nu}^2)}{(1-2\bar{\nu})}\frac{K}{\bar{K}}\omega\right]^{-1} \qquad (24)$$

Indeed (22) and (23) are formally the same as (17) and (18) with $(1 - \xi)$ replaced by D. Nevertheless, there are no simple equivalence rules relating the results for the partial saturation and soft-fluid saturation cases because D itself depends on $\bar{K}/K$. By combining the first equation of (22) with (24) we obtain an equation to be solved for D:

$$\epsilon D^2 - \left[\epsilon + \frac{9}{16}\frac{(1-2\bar{\nu})}{(1-\bar{\nu}^2)} + \frac{3\omega}{4\pi}\right]D + \frac{9}{16}\frac{(1-2\bar{\nu})}{(1-\bar{\nu}^2)} = 0 \qquad (25)$$

To solve (22) for the moduli given ϵ and ω, (23) and (25) must first be solved simultaneously for D and $\bar{\nu}$. The moduli can then be evaluated.

The results, again for $\nu = 1/4$, are shown in Figure 4 for various values of ω. Except for $\omega = 0$ the critical crack density parameter is always $\epsilon = 45/32$. At this point, both $\bar{E}$ and $\bar{G}$ vanish, but $\bar{K}$ attains the value

$$\frac{\bar{K}}{K} = (1 + 15\pi/8\omega)^{-1} \qquad (26)$$

It can be verified that for small c/a this result follows from a simple volume averaging of the compressibilities of the fluid and matrix materials.

The results for $\bar{K}/K$ and $\bar{G}/G$ in (22) agree with those of *Walsh* [1969] in the limit of small crack densities. A noteworthy feature of the results in Figure 4 is the nonuniform approach of the solution to that of the dry case as $\omega \to 0$. As a consequence the results for small nonzero ω are close to those for $\omega = 0$ only for $\epsilon < 9/16$; for larger ϵ they deviate significantly, a deviation that is most apparent for $\bar{\nu}$, which always eventually approaches 1/2 regardless of its initial trend.

Estimation of Crack Density

The crack density parameter ϵ is not amenable to direct measurement; it would be useful to have some method of estimating this parameter, such as by counting line segments formed by the intersections of the cracks with a plane section.

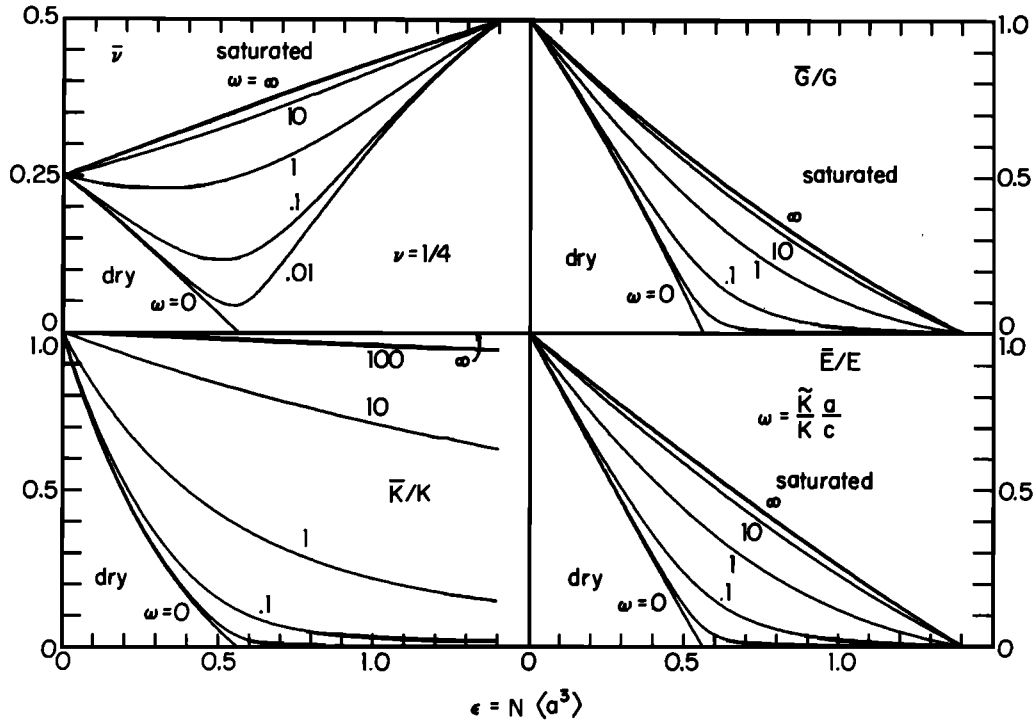

Fig. 4. Effective elastic properties of a solid permeated with circular cracks that are filled with a fluid of bulk modulus $\tilde{K}$. The crack aspect ratio (thickness/diameter) is c/a, and the important parameter is $\omega = (\tilde{K}/K)/(c/a)$. The case $\omega = 0$ corresponds to completely dry cracks, and $\omega = \infty$ to saturated cracks.

Such relations can in fact be found from considerations of geometrical probability.

In a plane section of a cracked solid, define the crack trace density M as the number of line segments per unit area. The crack trace length distribution $m(l)$ gives the observed variation of length of the cracks, and

$$M = \int_0^\infty m(l)\, dl$$

For cracks of any convex shape but uniform size one can show [*Kendall and Moran*, 1963] that

$$\epsilon = \frac{8}{\pi^3} M\langle l\rangle^2$$

where $\langle l\rangle$ is the mean length of crack traces observed. This result may be useful when the cracks are expected to be of fairly uniform size, such as grain boundary cracks in an equigranular rock.

For elliptic cracks of various sizes but uniform ellipticity $k = (1 - b^2/a^2)^{1/2}$ one can show [*Budiansky and O'Connell*, 1974] that

$$\epsilon = \frac{\pi^2}{4E(k)\,K(k)} \frac{3}{4\pi} M\langle l^2\rangle$$

where $K(k)$ and $E(k)$ are complete elliptic integrals (see appendix) and $\langle l^2\rangle$ is the mean of the length squared of the line segments. If there is a distribution of shapes and the size and shape distributions are uncorrelated, then we may average over k, and

$$\epsilon = \frac{\pi^2}{4} \langle 1/E(k)\,K(k)\rangle \frac{3}{4\pi} M\langle l^2\rangle \qquad (27)$$

where the angle brackets denote an average over all values of k. The function $\pi^2/[4E(k)K(k)]$ is shown in Figure 5 as a function of b/a. Only for very elliptical cracks ($b/a < 0.1$) does this function differ significantly from 1. A distribution of crack shapes would have to be very skewed toward small b/a for the average value of the function to differ from 1 by a large amount. Thus the crack trace density and mean (or mean square) length may be very good estimators of the crack density.

Elastic Wave Velocities

The velocities of shear and compressional elastic waves can

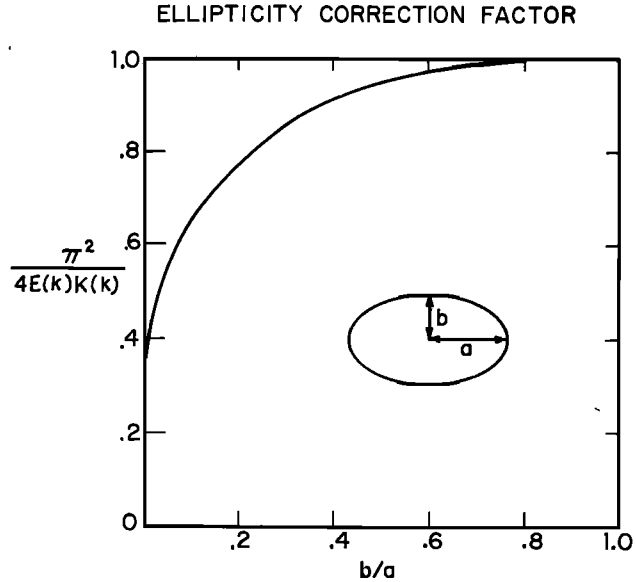

Fig. 5. The ellipticity correction factor as a function of crack ellipticity b/a. The factor relates the mean square length of line segments formed by the intersection of cracks with a thin section to the crack density that enters the relations for elastic properties; the exact relation is given by (27).

be obtained directly from the expressions for the effective moduli for any of the cases treated above.

The results for the shear wave velocity V_S, the compressional wave velocity V_P, and the ratio of the velocities V_P/V_S may be expressed by

$$\frac{\bar{V}_S}{V_S} = \left(\frac{\bar{G}}{G}\right)^{1/2}$$
$$\frac{\bar{V}_P}{V_P} = \left[\frac{(1-\bar{\nu})(1+\nu)}{(1+\bar{\nu})(1-\nu)}\frac{\bar{K}}{K}\right]^{1/2} \tag{28}$$
$$\frac{\bar{V}_P/\bar{V}_S}{V_P/V_S} = \left[\frac{(1-\bar{\nu})(1-2\nu)}{(1-2\bar{\nu})(1-\nu)}\right]^{1/2}$$

For the case of dry circular cracks the result for $\bar{V}_P$ agrees with that of *Garbin and Knopoff* [1973] for small crack densities, for which a non-self-consistent calculation may be used.

The effective wave velocities for the case of partial saturation, calculated from (17), (18), and (28), are shown in Figure 6 for different values of ξ. The presence of cracks, whether dry or saturated, results in a reduction of both velocities although by different amounts. For completely dry cracks ($\xi = 0$), both wave velocities decrease uniformly to zero (as the moduli do); however, the P wave velocity initially decreases about 40% more rapidly than the S wave velocity. For the completely saturated case ($\xi = 1$) the two velocities again decrease uniformly, but only the S wave velocity approaches zero. The P wave velocity decreases to a finite final value that is about 75% of its initial value. For this case the S wave velocity initially decreases about twice as fast as the P wave velocity, in contrast with the dry case in which the P wave velocity decreases more rapidly. These trends are apparent in the plot of $(\bar{V}_P/\bar{V}_S)/(V_P/V_S)$. Note that by (28), changes in this ratio for small ϵ are proportional to changes in Poisson's ratio, which increases for saturated cracks and decreases for dry cracks. Thus on such a plot the two cases are clearly discriminated in a manner much clearer than they are on the individual plots of $\bar{V}_P$ and $\bar{V}_S$.

For intermediate states of saturation, both velocities vanish for values of ϵ between 9/16 and 45/32. If two thirds of the cracks are saturated, the $\bar{V}_P/\bar{V}_S$ ratio is essentially constant; it decreases if more of the cracks are dry and increases if more of the cracks are saturated. Only for the completely saturated case does $\bar{V}_P/\bar{V}_S \to \infty$; for all other cases it remains bounded.

The velocities for the case of saturation with a 'soft fluid' (i.e., $\omega = (\bar{K}/K)(a/c) \sim 1$) are shown in Figure 7. For small crack densities ($\epsilon < 0.5$) the curves are similar to those of the previous case of partial saturation. For larger ϵ the two cases differ significantly (the two cases cannot be made equivalent by a transformation of parameters, as has been mentioned previously). For all values of $\omega > 0$ the shear velocity eventually vanishes at $\epsilon = 45/32$, whereas the P velocity reaches a finite value corresponding to the final value of $\bar{K}/K$ given by (26).

The relative changes in the velocities is again best seen in the plot of $(\bar{V}_P/\bar{V}_S)/(V_P/V_S)$. For ω around 1 this ratio is essentially constant for values of crack density less than 0.6. This value of ω corresponds to the case when the aspect ratio of the crack is equal to the ratio of the fluid and solid bulk moduli. For more compressible fluids (or thicker cracks) the velocity ratio will be more similar to the dry case and will decrease. Conversely, for less-compressible fluids (or thinner cracks) the behavior will be more like that for saturated cracks with $\omega = \infty$. In general, the results for saturated cracks depend on the bulk modulus of the fluid and the aspect ratio of the cracks, and for all but the empty case ($\omega = 0$), the velocity ratio eventually increases and approaches infinity as $\epsilon \to 45/32$.

DISCUSSION

The model that we have analyzed consists of a solid permeated with randomly oriented elliptical cracks. The ques-

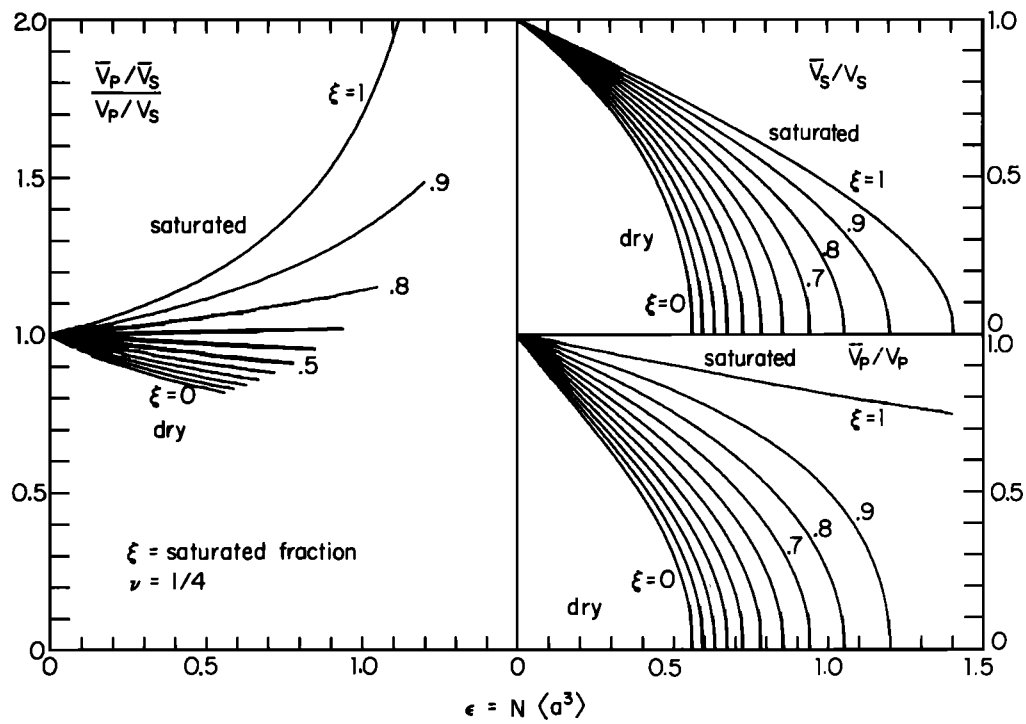

Fig. 6. Effective shear wave velocity $\bar{V}_S/V_S$, compressional wave velocity $\bar{V}_P/V_P$ and velocity ratio $(\bar{V}_P/V_P)/(\bar{V}_S/V_S)$ for a partially saturated cracked solid. The fraction of saturated cracks is ξ. The wave velocities correspond to the moduli shown in Figure 3.

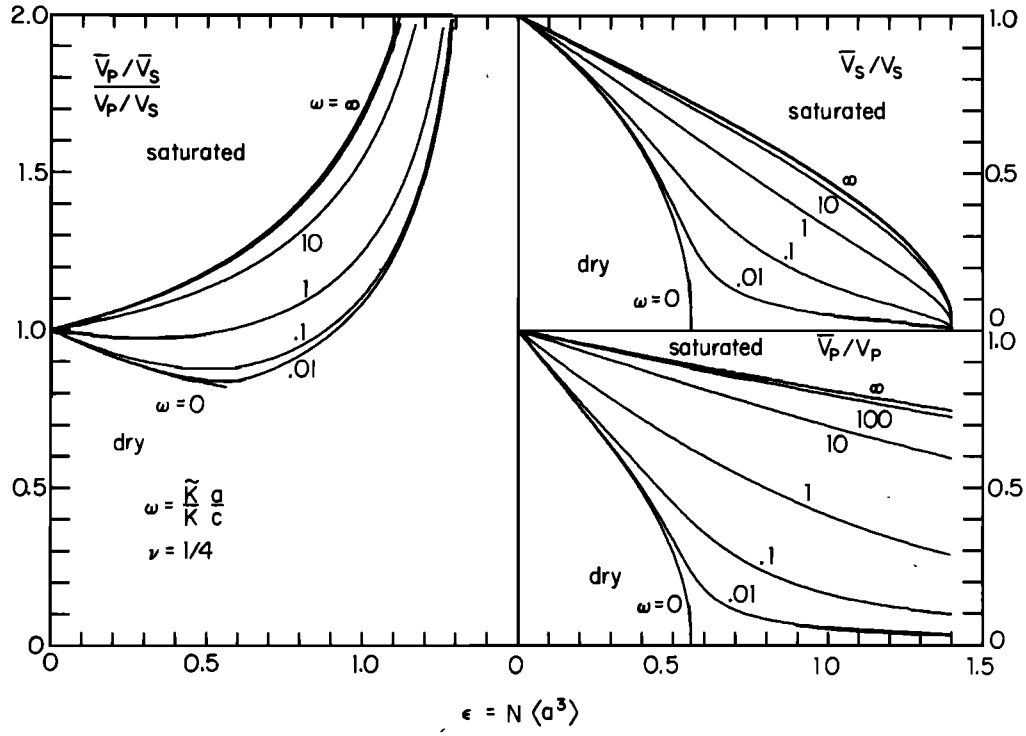

Fig. 7. Effective wave velocities $\bar{V}_S/V_S$ and $\bar{V}_P/V_P$ and their ratio for a solid with cracks of aspect ratio c/a, all filled with a fluid of bulk modulus $\tilde{K}$. The corresponding moduli are shown in Figure 4.

tion remains of how well real rocks actually conform to this model, so that our results might prove useful in analyzing or predicting their elastic properties. The fact that the calculated elastic properties do not depend on the ellipticity of the cracks leads us to expect that the crack shape may not be particularly important. The degree to which rocks are isotropic can of course be measured. The main question is the extent to which the self-consistent approximation takes into account accurately the interactions between cracks and whether the crack density in rocks is such that the details of crack intersections are important. These questions can be approached by comparison of our results with data on the elastic wave velocities measured on rock samples.

Crack densities have generally not been measured or estimated. For the purpose of examining data on V_P and V_S we may plot the ratio V_P/V_S against V_S, which is suggested by the monotonic dependence of V_S on ϵ. Such a plot is shown in Figure 8 for the case of partial saturation. Figure 9 is a similar plot for the soft-fluid saturated case. Contours of constant crack density ϵ are shown on each figure as well as curves for different values of either ξ or ω. The curves for the limiting values of dry cracks ($\omega = 0$ or $\xi = 0$) and saturated cracks ($\omega = \infty$ or $\xi = 1$) on each figure are identical. The contours of constant crack density also are the same for both figures. Thus measurement of any two of V_P, V_S, or V_P/V_S specifies a point on either plot that uniquely determines the crack density regardless of whether one interprets the data in terms of partial saturation (Figure 8) or the properties of the fluid and the crack shape (Figure 9). Depending on which interpretation is chosen, a point on either plot also specifies either the degree of saturation ξ or the value of ω. From the value of ω, either the aspect ratio c/a or bulk modulus of the fluid can be determined if the other is known. The aspect ratio can be estimated if the crack porosity η is known, since $\eta/\epsilon = (4\pi/3)(c/a)$.

The data of *Nur and Simmons* [1969] are shown in Figure 10 as a normalized plot of $\bar{V}_P/\bar{V}_S$ against $\bar{V}_S$. The data were obtained by measuring wave velocities in both dry and saturated rock samples at various pressures up to 3 kbars. The effect of pressure was presumably to vary the crack density by squeezing cracks shut. The velocities of the uncracked body were assumed to be those observed at the highest pressure in each experiment. Also shown are the theoretical curves for the two limiting cases of dry cracks or fully saturated cracks. The values for ν used in those calculations were calculated from the velocities for the uncracked rocks used for normalization.

The dry Westerly granite data generally follow the theoretical curve except for the first two points (i.e., the points on the right, which were obtained at the lowest pressures). This situation could be due to anisotropy, errors in the measurements of V_P and V_S (V_P too low or V_S too high), or to the inadequacy of the theory. Nevertheless, the general agreement is quite good. The values for the saturated case fall somewhat below the theoretical curve, a situation that could be due to incomplete saturation of the rock, in which case 15% of the cracks were unsaturated, as can be seen from Figure 8. The fact that the data of *Takeuchi and Simmons* [1973] for the same rock (saturated) are closer to the theoretical curve supports this interpretation. For both cases the value of ϵ at zero pressure (i.e., for the rightmost points on the graph) is around 0.25, which is substantial, corresponding to one crack of radius 0.6 per unit volume (e.g., one crack with a diameter of 1.2 mm/mm^3). This large value of ϵ clearly illustrates the inadequacy of a theory for a sparse distribution of cracks and supports our use of a self-consistent theory.

The dry Casco granite data lie above the theoretical curve except for the point at lowest pressure on the right. (The points at $\bar{V}_S/V_S = 0.75$ and 0.83 are shown twice: the upper points are calculated from the data reported by *Nur and Simmons* [1969], and the lower points use the ratios reported by *Nur* [1972], which were obtained from the same data. In plotting the lower

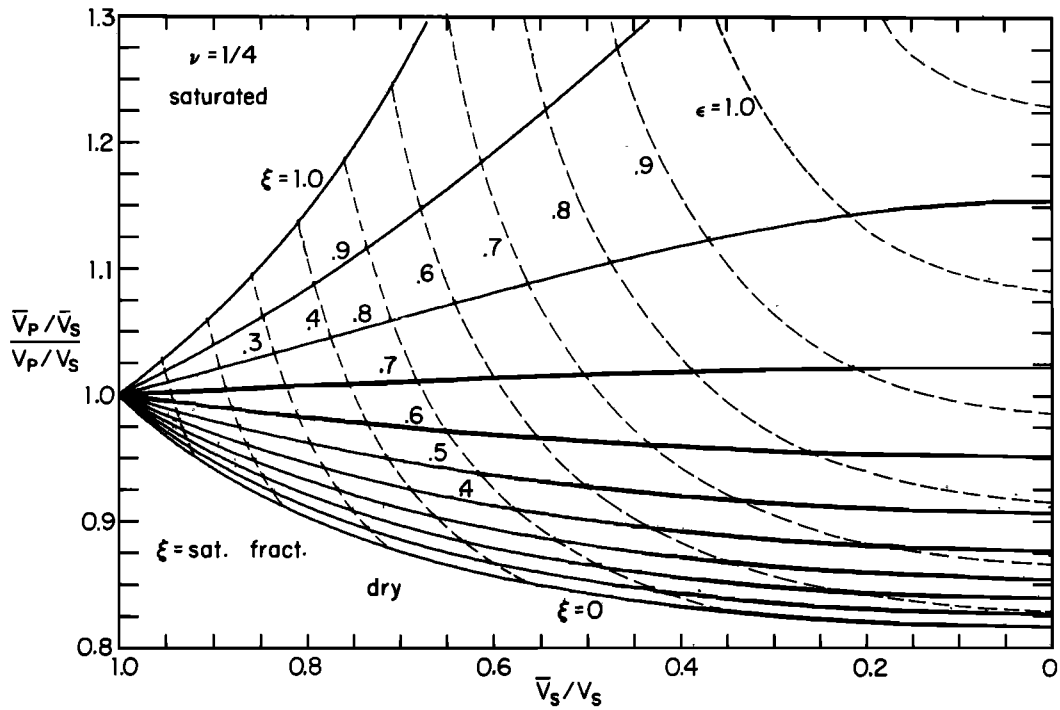

Fig. 8. The velocity ratio $(\bar{V}_P/\bar{V}_S)/(V_P/V_S)$ versus shear wave velocity $\bar{V}_S/V_S$ for a partially saturated cracked solid for several values of the saturated fraction ξ. Contours of constant crack density $\epsilon = N\langle a^3 \rangle$ are shown as dashed lines. Measurement of $\bar{V}_P/V_P$ and $\bar{V}_S/V_S$ for a real material specifies a point on this diagram from which both the crack density and degree of saturation may be determined.

points we have assumed that the V_S values are the same and that the discrepancy was in V_P.)

The departure of the dry data from the theoretical curve could be due to the presence of residual water in some of the cracks, so that as the cracks are squeezed shut, they eventually close down on the trapped water and behave as saturated cracks. The trend of the first three points is roughly along a line of constant crack density $\epsilon = 0.4$, the degree of saturation ξ increasing from zero to around 0.6. (cf. Figure 8). The remaining points indicate a reduction in crack density at a constant state of saturation $\xi \sim 0.6$.

The data for the wet case agree remarkably well with the

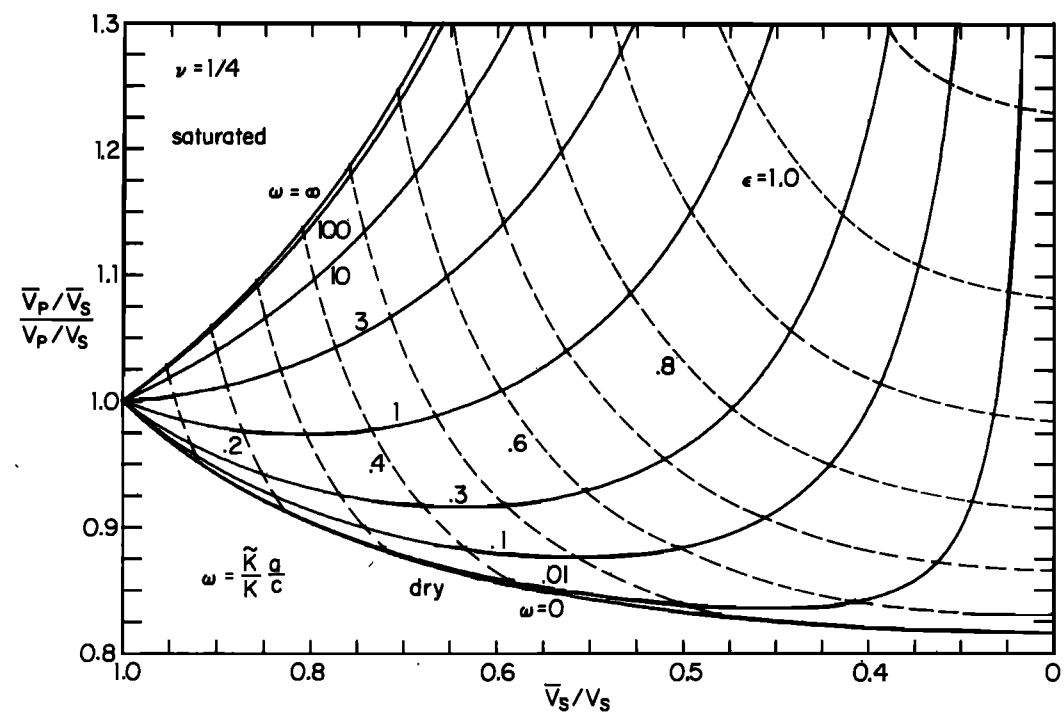

Fig. 9. Similar to Figure 8, but for the case of saturation of cracks of aspect ratio c/a with a fluid of bulk modulus $\tilde{K}$. The contours of constant crack density (dashed lines) are identical to those of Figure 8; thus determination of the crack density is independent of the choice of the model.

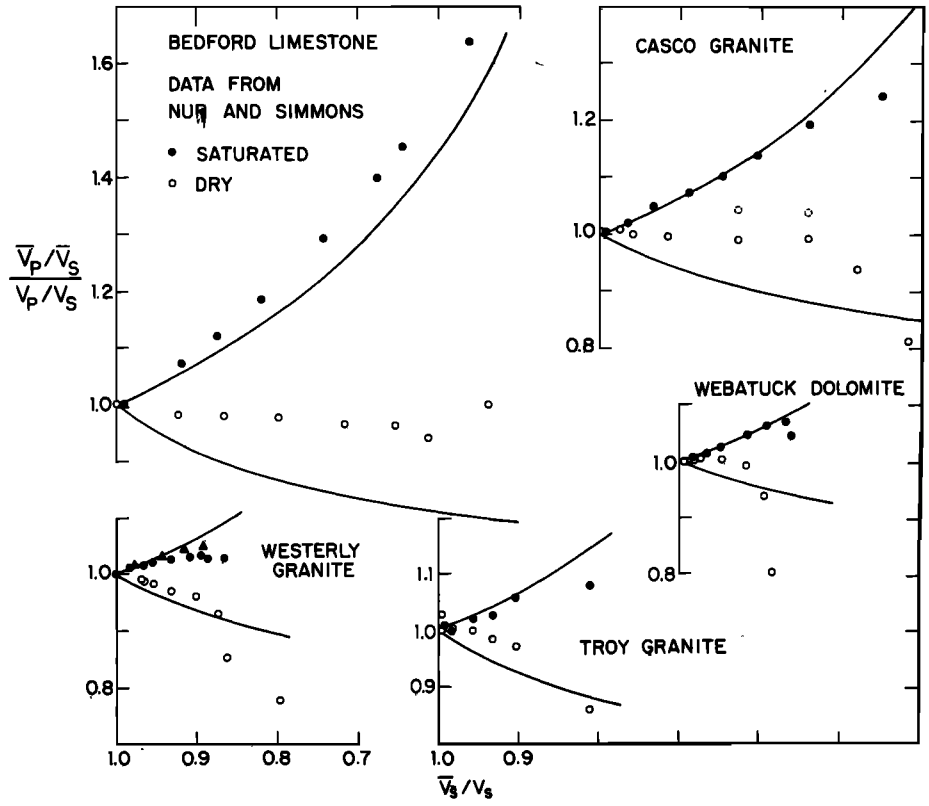

Fig. 10. Elastic wave velocities of rocks measured by *Nur and Simmons* [1969] plotted on diagrams similar to Figures 8 and 9. The data are for both dry (open circles) and saturated samples (solid circles); the data of *Takeuchi and Simmons* [1973] for a saturated Westerly granite sample are shown as triangles. The two extra points (dashed circles) for Casco granite are discussed in the text. The theoretical curves from Figure 8 or 9 for either completely dry or saturated cracks are also shown.

theory. The maximum crack density for the wet case is $\epsilon \sim 0.7$; this is higher than the value for the dry case, perhaps a result of the introduction or extension of cracks during the process of saturating the rock. The maximum crack density for both cases is quite large and is in a range where the statistics of crack intersection might be considered important. However, the agreement between the data and the present theory for such large values of ϵ lends confidence in the self-consistent approximation.

For Troy granite the data for the dry case follow a trend similar to that of the data for Westerly granite, and the data for the wet case agree very well with the self-consistent theory. The data for Webatuck dolomite are similar. The first two dry points are anomalously low; the data for the saturated case agree quite well with theory. The data for Bedford limestone follow very consistent trends. For the saturated case they agree well with the theory. The fact that the points are somewhat above the curve may be due to normalization, which is suggested by the large variation in V_S and V_P/V_S even up to the highest pressure (2 kbar) represented by the points on the left. The data for the dry case lie between the curves for completely dry and saturated rocks and correspond to a degree of saturation $\xi \sim 0.6$. We should note that this rock has significant porosity not associated with cracks, which may account for some of the differences between data and theory.

From crack porosities η for dry samples reported by Nur and Simmons and the formula $c/a = 3\eta/4\pi\epsilon$ we can estimate aspect ratios c/a using values of ϵ inferred by comparisons of the data plots in Figure 10 with Figure 8 or 9; these are tabulated in Table 1. The aspect ratios are of the order of 0.001, which is consistent with the observation that a pressure of only a few kilobars is sufficient to close most of the cracks and raise the velocities near the intrinsic values for uncracked rocks. The crack density for all the rocks is rather high, $\epsilon \sim$ 0.2–0.6, implying one crack of greater than unit diameter per unit volume. The rocks are thus extensively cracked, and we might expect that a modest increase in crack density would render the rocks extremely fragile. Such an increase would not require the extension of cracks by much; small extensions that resulted in the joining of cracks would suffice to increase the crack density substantially, as was mentioned previously.

EARTHQUAKE PRECURSORS

The variations in the arrival times of seismic waves preceding earthquakes, reported by Soviet seismologists, have been interpreted by *Nur* [1972] as being due to variations in the density and state of saturation of cracks present in the rocks

TABLE 1. Inferred Crack Densities and Aspect Ratios

Rock	Crack Porosity	ϵ (dry)	c/a (dry)
Westerly granite	0.002	0.25	0.0015
Casco granite	0.0045	0.4	0.002
Troy granite	0.001	0.25	0.0008
Webatuck dolomite	0.0022	0.15	0.003
Bedford limestone	0.002	0.6	0.0007

Crack porosities from the paper by *Nur and Simmons* [1969] and crack densities from Figures 8 and 10 were used.

near the focal zone of the earthquake. The observation indicated that the ratio V_P/V_S decreased and remained low for some period (1–3 months) before moderate earthquakes and increased to normal values just before the earthquake. Nur proposed that the decrease was due to the opening of new dry cracks around the focal zone of the earthquake, which reduced the observed seismic velocities. *Whitcomb et al.* [1973] pointed out that vaporizing the fluid in saturated cracks would have the same effect. This state persisted until enough water diffused into the dilated region to fill the newly expanded cracks and raise the pore pressure. The increased pore pressure weakened the rock, the result being eventual failure evidenced by the earthquake.

Observations similar to those reported in the Soviet Union have been made by *Aggarwal et al.* [1973] for small earthquakes and by *Whitcomb et al.* [1973] for a larger earthquake, the San Fernando earthquake of February 9, 1971, which had a magnitude of 6.4. For this latter case the arrival times of both P and S waves were measured, and calculated values of V_P and V_S reported. If the observed variations are indeed due to variations in the degree of saturation and density of cracks, we may use a plot of V_P/V_S versus V_S (e.g., Figures 8 and 9) to investigate these variables, as was done above for the laboratory data on rock samples.

Figure 11 shows the velocity data of *Whitcomb et al.* [1973] obtained from recording the arrival times of both P and S waves at the stations PAS (Pasadena, California) and RVR (Riverside, California) from small earthquakes near the San Fernando aftershock area, as shown in Figure 11*c*. Also shown are data from the paper by *Anderson and Whitcomb* [1974] from travel times to the stations PAS and SWM (Sawmill, California) for earthquakes south or west of PAS, all well outside of the aftershock zone. Each of the calculated velocities marked PAS-SWM must represent some average velocity in the region between the two stations PAS and SWM; a similar interpretation applies to the PAS-RVR velocities. For the PAS-RVR data this region is primarily between the stations PAS and RVR, which is well outside of the aftershock area. In contrast, the PAS-SWM region includes the aftershock zone.

The last 10 data for PAS-RVR are shown in Figure 12, plotted on a figure of $(\bar{V}_P/\bar{V}_S)/(V_P/V_S)$ against $\bar{V}_S/V_S$, reproduced from Figure 8. The data have been normalized to the highest observed velocities, $V_P = 7.4$ and $V_S = 4.3$ km/s, measured in 1962. The time sequence of the data is indicated by numbers that correspond to those in Figure 11. Before the decrease in $\bar{V}_P/\bar{V}_S$ in 1967 the data (points 1–6) are generally in the region $\epsilon = 0.2$–0.3 and $\xi = 0.8$–1.0. In view of the estimated errors of the data shown in Figure 11 and the different paths for different earthquakes, no significance can be placed on the detailed variations; nevertheless, it is clear that the data correspond to predominantly saturated cracks of density $\epsilon \sim 0.2$. There is the further indication from the inferred value of ξ that most of the cracks are saturated. Alternatively, it could be (cf. Figure 9) that $\omega \sim 10$ and that the saturating fluid has a bulk modulus somewhat lower than water or the aspect ratio of the cracks is large. We shall assume the first model, that of partial saturation, for the purpose of discussion; we shall see that the conclusions to be drawn do not depend on this particular choice.

The decrease in $\bar{V}_P/\bar{V}_S$ in 1967 (points 6–7) occurs at essentially constant crack density and indicates the introduction of a low-modulus vapor phase in all of the cracks that were previously completely filled with fluid. This is consistent with the interpretation of *Whitcomb et al.* [1973]. The subsequent

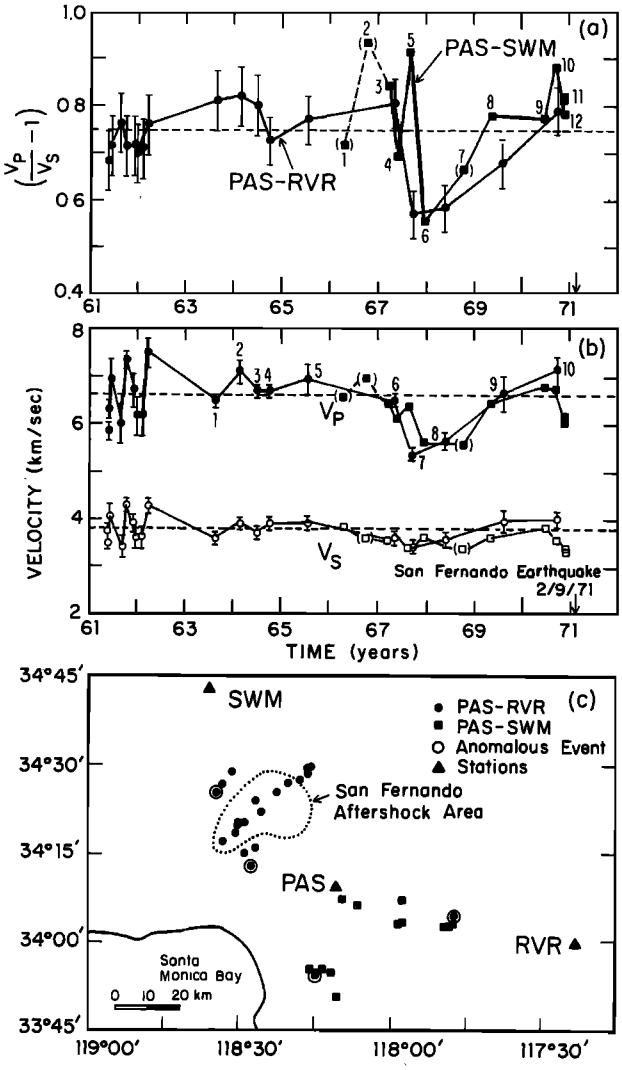

Fig. 11. Average wave velocities prior to the San Fernando earthquake reported by *Whitcomb et al.* [1973] and *Anderson and Whitcomb* [1974]. The lowest panel shows the locations of the events and stations used to obtain the velocities. The PAS-SWM velocities were obtained from events (shown as squares) that were observed at the stations PAS and SWM. The PAS-RVR velocities came from events in the aftershock area (circles) recorded at PAS and RVR. The events during the period of low V_P/V_S in 1967 and 1968 are circled.

increase of $\bar{V}_P/\bar{V}_S$ (points 7–10) indicates a reduction in crack density from 0.25 to 0.15 and resaturation of the cracks. This reduction in crack density is counter to the hypothesis of increased dilatancy upon resaturation and implies rather a relaxation of strain, which allows some cracks to close completely while the remainder relax sufficiently to eliminate the vapor phase present within them.

The region to which the PAS-RVR data apply is away from the epicentral zone; thus the observed reduction in crack density may not be indicative of the processes near the fault that lead to failure. The epicentral region may possibly be investigated by looking at the PAS-SWM data in Figure 12, which corresponds to paths traversing the aftershock area. As was noted before, the detailed variations may be due to errors, which are presumably about the same as those for the PAS-RVR data, and to the effect of different paths for different shocks, which may be greater for this region if large changes in $\bar{V}_P$ and $\bar{V}_S$ take place immediately within the epicentral region. Prior to the decrease in $\bar{V}_P/\bar{V}_S$ (points 2–3) in 1967, the data

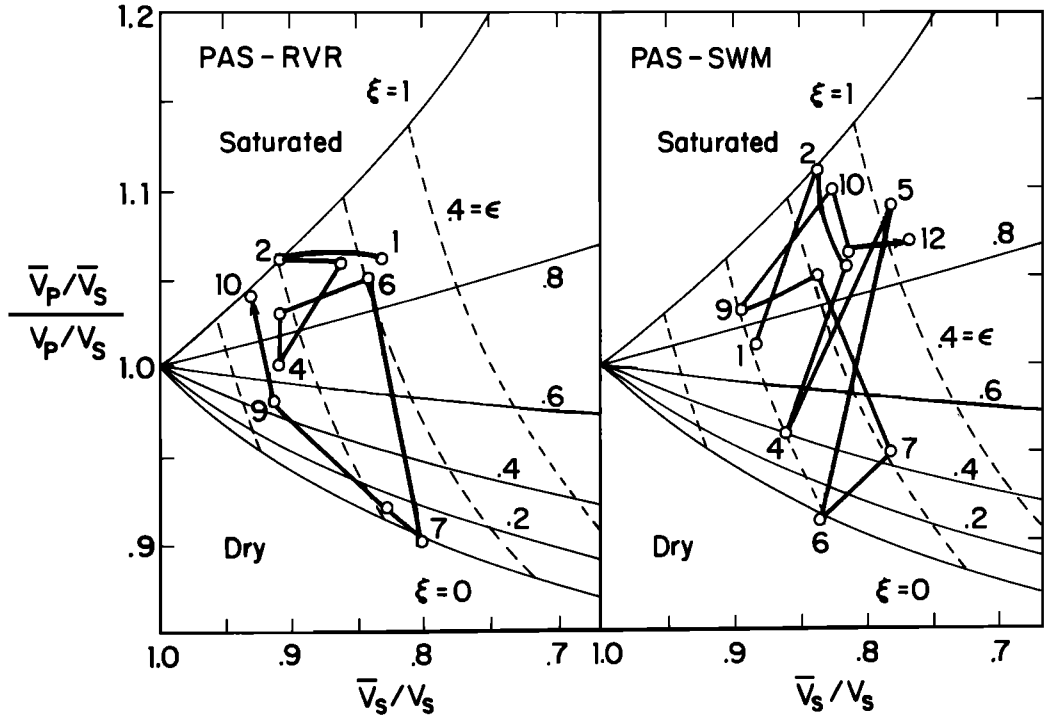

Fig. 12. The velocity data of Figure 11 plotted on a diagram like Figure 8. The crack density ϵ and degree of saturation ξ are indicated. The data are sequentially numbered, corresponding to the numbers in Figures 11*a* and 11*b*. The history of crack density and saturation can be seen for each region. The drop in V_P/V_S was due to a change from saturated ($\xi \sim 1$) to dry cracks ($\xi \sim 0$) at constant crack density $\epsilon \sim 0.3$. Subsequently, both regions resaturate, PAS-RVR with decreasing crack density and PAS-SWM with increasing crack density.

again imply mostly saturated cracks. The indicated crack density is slightly higher than it was for the previous case, an observation that may be characteristic of the region near the epicenter. A decrease in crack density accompanies the decrease in $\bar{V}_P/\bar{V}_S$ (points 3–4); this effect is more marked than it was for the other case. (The increase and subsequent decrease in $\bar{V}_P/\bar{V}_S$ at points 4, 5, and 6 may be a path effect, which may be worth investigating in detail.) The increase in $\bar{V}_P/\bar{V}_S$ (points 6–7) does not follow the same trend as it did in the previous case; rather an increase in crack density accompanies the V_P/V_S increase. This different trend persists; the final data correspond to higher crack densities than those that existed before the earlier decrease in $\bar{V}_P/\bar{V}_S$. The last points show a drop in both $\bar{V}_P$ and $\bar{V}_S$ and an increase in ϵ, a situation that is in complete accord with the hypothesis of crack growth upon resaturation leading to failure, as was originally proposed by Nur.

Thus although the observed velocity variations in the two regions are grossly similar, their detailed consideration in terms of the theory suggests significant differences between the two regions. In particular, the data for the epicentral region are consistent with the hypothesis of dilatancy, resaturation, and then further dilatancy, whereas the data for a region away from the epicenter, which also show a precursory drop in $\bar{V}_P/\bar{V}_S$, follow a different trend, namely, dilatancy, resaturation, and then relaxation. These differences may be related to the processes leading up to the earthquake and may be indicative of the temporal and spatial variations in the elastic state of the region. It is therefore of interest to explore some of the implications of the changes in crack properties indicated by the velocity data with regard to the regional stress and the elastic properties of the rock.

The elastic state (i.e., stress and strain) of the rock and the state of the cracks are interrelated in several ways. (1) Cracks reduce the effective elastic moduli of the rock; i.e., they permit a larger strain for a given stress than what would be the case with no cracks. (2) Changes in stress can vary the crack density by opening closed cracks or completely closing open cracks; open cracks can be extended by fracture; consequently, the moduli are affected. (3) Opening of cracks can reduce the pressure of the pore fluid [*Anderson and Whitcomb*, 1973, 1974], changing its elastic properties (e.g., vaporization), which in turn affects the moduli of the rock; conversely, partial closure of cracks containing fluid and vapor can produce saturated cracks by eliminating the vapor phase. (4) Changes in pore pressure can close, open, or extend cracks. (5) Changes in strain can in turn vary the pore fluid pressure by changing the crack volume. (6) Changes in crack density and thickness of cracks can vary the permeability of the rock and hence the spatial distribution of the pore fluid pressure and properties.

The interrelation between regional stress and strain, crack density and volume, and fluid properties is complex, as is the relation of these variables to strain accumulation and faulting. Nevertheless, there are several characteristics of the San Fernando velocity data that may be interpreted readily. These are the state of both regions before the drop in V_P/V_S, the drop in V_P/V_S, and the nature of and the differences between the two regions in the recovery of V_P/V_S to previous values. We shall discuss each of these in turn.

For some time before the decrease in V_P/V_S in 1967 the rocks in both regions contained a substantial number of cracks ($\epsilon \sim 0.2$). The average crack density would be expected to have changed slowly as a result of changes in tectonic stresses; in addition, there would have been spatial variations about this average owing to geologic inhomogeneities and short-term temporal variations associated with small earthquakes. These

cracks apparently existed stably in the ambient stress field, and most of them were saturated with fluid. Changes in the regional stress field would vary the thicknesses of cracks, causing some to open and others to close. The detailed mechanism of changes in crack density and thickness due to stress can be complex and is, at present, not known, but it is not difficult to imagine processes in which the number of cracks opening would exceed the number closing and there would be a net increase in crack volume. This in turn would lower the pressure of the pore fluid to the extent that it would vaporize, and the cracks would then behave as dry cracks in response to seismic waves.

The decrease in V_P/V_S in both regions clearly corresponded to a change from saturated cracks to dry cracks. There is no indication of the formation of new dry cracks, in which case the crack density would have increased. In fact, it decreased a little, if anything. The decrease in V_P/V_S could have been due to the introduction of a vapor phase into nearly all the cracks. Another interpretation of the drop in V_P/V_S is that the value of ω changed owing to a large change in the aspect ratio. For example, if $\tilde{K}/K = 3 \times 10^{-4}$ and if c/a changed from 10^{-5} to 10^{-2}, then the observed velocity changes would be accounted for. The most plausible explanation is a combination of both effects, namely, c/a increasing and $\tilde{K}/K$ consequently decreasing as a result of the reduction of pore pressure. It is not possible to determine the relative magnitude of each effect without independent information about the pore pressure or amount of dilatancy.

A most striking phenomenon is that the decrease in V_P/V_S occurred over a region much larger than the epicentral region, as has been noted by *Anderson and Whitcomb* [1974]. This observation is compounded by the transition from saturated to essentially completely unsaturated cracks over the entire region with no change in crack density. The indicated crack densities are such that the velocity reduction must have been distributed over the whole region and not have been due to a localized anomalous zone. If such were the case, the crack density in the region would have to be considerably higher and near the value for which failure might be imminent.

The recovery of the velocities to previous values is distinctly different for each of the two regions. The behavior for the PAS-RVR region indicates a reduction in crack density and resaturation; the final state is again saturated, but the density is less than it was before the process started, although it is still finite. This behavior could be a result of the relaxation of the stress that caused the initial dilation, so that the cracks relaxed to their former thicknesses in which state they were saturated. The reduction in crack density suggests that the pore volume might have been less than before, in which case the pore fluid would have flowed to an adjacent region (which could have been directly above).

An alternative explanation is that the cracks were squeezed shut by an increase of properly oriented stresses. As they closed, the residual fluid was eventually sufficient to resaturate them; further closing may have forcibly expelled fluid into adjacent regions; again the fluid flow could have been either vertical or horizontal. For either alternative a net reduction in pore volume would be expected to accompany the decrease in crack density. A decrease in permeability would also be expected.

The decrease in crack density would result in an increased stiffness for the rock in the region based on the relations between elastic moduli and crack density. The internal pore pressure would presumably be greater than it was in the dilatant state; nevertheless, the fact that the crack density decreased indicates an increase in effective pressure (external pressure minus pore pressure), which would also tend to strengthen the rock. (In fact, the proper relation between effective pressure and strength or elastic stiffness of a cracked solid is partly through the relation between effective pressure and crack density.)

In the region PAS-SWM, which includes the epicentral region, the implied changes in the cracks during the recovery of V_P/V_S are distinctly different than those in the other region. The epicentral region did not exhibit a decrease in crack density during resaturation; rather it remained roughly constant. After the cracks became completely resaturated, there was a decrease in saturation and then a marked increase in crack density that appeared to accelerate just before the earthquake.

During resaturation at constant crack density there would be an increase in pore pressure, which would have permitted an increase in crack thickness and pore volume. This in turn would have increased the permeability of the rock. The effective pressure may have decreased to a level that permitted the extension of existing cracks or the formation of new dry cracks by fracture, which resulted in the increase in crack density; in either case there would have been a net dilation of the entire region. The rock would have been weakened by the increase in crack density; it may have been weakened to the extent that permitted further crack growth in the existing stress field. Such a process could have culminated in the earthquake.

The fact that the crack history for the two regions is different implies that other related phenomena would be different. After both regions experienced dilation at the time of the initial V_P/V_S drop, the epicentral region would have continued to dilate. As water flowed into the dilated cracks, the local water table may have dropped. There would also have been an accelerating uplift of ground level as the crack density increased, creating more pore volume and weakening the rock and permitting existing cracks to dilate further. The increase in crack density may have been accompanied by an increased number of microseisms.

The surrounding region, on the other hand, would have exhibited a contraction following the initial dilation. As open cracks closed, there would have been a drop in ground level. The local water table would have risen as pore fluid was expelled from the closing cracks. The number of microseisms may have decreased owing to the absence of crack extension and the stiffening of the rock caused by the decrease in crack density. During such a process the boundary between the two regions may not be stationary but might move toward the epicentral region as the strain accumulates; tilts near the boundary would be large, and their variation should reflect the movement of the boundary. The history of a small region through which the boundary migrates would be more complex. The period of initial dilation, uplift, and dropping water table would be followed by subsidence and a rising water table. Observation of such effects may be indicative of the proximity in both space and time of an earthquake.

The important conclusions from comparing the San Fernando data with the theory are that the rocks over a large region were extensively cracked and saturated, that the decrease in V_P/V_S was due to a change from saturated cracks to dry cracks and not to the formation of new cracks, that the epicentral region became more cracked after resaturation, that the nonepicentral region became less cracked as it became resaturated, and that the variation in effective stress, permeability, pore pressure, rock stiffness, and strength may

have been quite different for the two regions. Changes in these conclusions will require either new data or a theory that includes effects that we have not considered, most importantly anisotropic crack distributions and stresses. In any event, interpretations based on the present theory are clearly sounder than those based directly on *Nur and Simmons*'s [1969] laboratory data or *Walsh*'s [1969] theory for a sparse crack concentration, both of which are consistent with the present theory as has been shown.

CONCLUSIONS

The expressions that we have presented for the elastic moduli of a cracked solid are relatively simple and permit straightforward evaluation. The results obtained are physically reasonable even for limiting values of the crack density; for smaller crack densities the results should be quite reasonable, as is borne out by the agreement with laboratory measurements. The most important parameter is the crack density ϵ; this parameter depends only on the area and perimeter of the cracks and not on the thickness, and hence it is independent of the crack or pore volume. For either dry or water-saturated cracks this is the only parameter that determines the elastic properties. The effect of crack thickness (or aspect ratio) enters only through the parameter $\omega = (\tilde{K}/K)/(c/a)$, which also determines whether or not the cracks may be regarded as being dry ($\omega < 0.1$) or saturated ($\omega > 10$). Thus it is not possible to determine separately either the fluid bulk modulus $\tilde{K}$ or the crack aspect ratio without knowing the other. A mixture of dry and saturated cracks gives results similar but not equivalent to saturation with a fluid such that ω is neither very large nor small in comparison with unity. It is not possible to determine from the observed elastic properties which of the cases of partial saturation or of soft-fluid saturation actually holds. Nevertheless, the crack density may be determined uniquely regardless of the interpretation of the state of saturation. In addition, it may be estimated directly by directly observing crack traces in plane sections.

The comparison of the theoretical results with laboratory measurements showed generally good agreement except for discrepancies that could be explained plausibly. In general, these indicated that 'dry' laboratory samples of rock contained residual water in at least some cracks. This may indicate that not all the cracks are connected, so that attempts to dry or saturate a bulk sample may not in fact dry or saturate all the cracks. The crack densities of some saturated samples were larger than those of the dry samples; this observation may indicate that the process of saturation can increase the crack density. This would tend to complicate the interpretation of laboratory measurements. The aspect ratios of the cracks in the dry samples were all about 10^{-3}.

The comparison of observed variations of seismic velocities before an earthquake with the theory showed that one can interpret such data directly in terms of changes in crack density and the state of saturation of the cracks. This result should be a very useful tool in analyzing other such data. The data for the San Fernando earthquake indicated that a large region surrounding the epicenter was extensively cracked and that the observed changes in V_P/V_S were primarily due to changes in the state of saturation of the cracks rather than in the number of cracks. This result suggests that a large number of cracks exist at considerable depth in the crust and that over a large region the fluid saturating the cracks can vaporize [*Anderson and Whitcomb*, 1973, 1974] and thus markedly affect the elastic properties of the region.

APPENDIX

The complete elliptic integrals referred to in the text are

$$E(k) \equiv \int_0^{\pi/2} (1 - k^2 \sin^2 \varphi)^{1/2}\, d\varphi \qquad \text{(A1)}$$

$$K(k) \equiv \int_0^{\pi/2} (1 - k^2 \sin^2 \varphi)^{-1/2}\, d\varphi \qquad \text{(A2)}$$

where $k \equiv (1 - b^2/a^2)^{1/2}$.

The function $T(b/a, \bar{\nu})$ appearing in the results for elliptical cracks (equations (10)–(12)) is

$$T(b/a, \bar{\nu}) = k^2 E(k)\{[(k^2 - \bar{\nu})E(k) + \bar{\nu}k_1^2 K(k)]^{-1} + [(k^2 + \bar{\nu}k_1^2)E(k) - \bar{\nu}k_1^2 K(k)]^{-1}\} \qquad \text{(A3)}$$

where $k_1 = (1 - k^2)^{1/2} = b/a$.

The algorithm of *Bulirsch* [1969] is particularly useful for evaluating (A3) as $k \to 0$, for which (A3) becomes indeterminate.

Acknowledgments. This work was supported by National Science Foundation grants NSF GP 34723 and NSF GH 33576 and the Committee for Experimental Geology and Geophysics of Harvard University. We thank Don L. Anderson and J. Whitcomb for a preprint and permission to use data before publication.

REFERENCES

Adams, L. H., and E. D. Williamson, The compressibility of minerals and rocks at high pressures, *J. Franklin Inst., 195,* 475–529, 1923.

Aggarwal, Y. P., L. R. Sykes, J. Armbruster, and M. L. Sbar, Premonitory changes in seismic velocities and prediction of earthquakes, *Nature, 241,* 101–104, 1973.

Anderson, D. L., and J. H. Whitcomb, The dilatancy diffusion model of earthquake prediction, in *Proceedings of the Conference on Tectonic Problems of the San Andreas Fault System,* edited by R. L. Kovach and A. Nur, pp. 417–426, Stanford University Press, Stanford, Calif., 1973.

Anderson, D. L., and J. H. Whitcomb, Time-dependent seismology, submitted to *J. Geophys. Res.,* 1974.

Birch, F., The velocity of compressional waves in rocks to 10 kilobars, 1, *J. Geophys. Res., 65,* 1083–1102, 1960.

Birch, F., The velocity of compressional waves in rocks to 10 kilobars, 2, *J. Geophys. Res., 66,* 2199–2224, 1961.

Brace, W. F., E. Silver, K. Hadley, C. Goetze, Cracks and pores: A closer look, *Science, 178,* 162–169, 1972.

Budiansky, B., and R. J. O'Connell, Elastic moduli of a cracked solid, submitted to *Int. J. Solids Struct.,* 1974.

Bulirsch, R., Numerical calculation of elliptic integrals and elliptic functions, 3, *Numer. Math., 13,* 305–315, 1969.

Eshelby, J. D., The determination of the elastic field of an ellipsoidal inclusion and related problems, *Proc. Roy. Soc. London, Ser. A, 241,* 376–396, 1957.

Garbin, H. D., and L. Knopoff, The compressional modulus of a material permeated by a random distribution of circular cracks, *Quart. Appl. Math., 30,* 453–464, 1973.

Kendall, M. G., and P. A. P. Moran, *Geometrical Probability,* pp. 78–84, Charles Griffin, London, 1963.

Kirkpatrick, S., Percolation and conduction, *Rev. Mod. Phys., 45,* 574–588, 1973.

Nur, A., Dilatancy, pore fluids and premonitory variations of t_s/t_p travel times, *Bull. Seismol. Soc. Amer., 62,* 1217–1222, 1972.

Nur, A., and G. Simmons, The effect of saturation on velocity in low porosity rocks, *Earth Planet. Sci. Lett., 7,* 183–193, 1969.

Shankland, T. J., and H. S. Waff, Conductivity in fluid-bearing rocks, *J. Geophys. Res., 79,* 4863–4868, 1974.

Simmons, G., and A. Nur, Granites: Relation of properties in situ to laboratory measurements, *Science, 162,* 789–791, 1968.

Spetzler, H., E. Schreiber, and R. J. O'Connell, Effect of stress-induced anisotropy and porosity on elastic properties of polycrystals, *J. Geophys. Res., 72,* 4938–4944, 1972.

Takeuchi, S., and G. Simmons, Elasticity of water-saturated rocks as a function of temperature and pressure, *J. Geophys. Res., 78,* 3310–3320, 1973.

Walsh, J. B., The effect of cracks on the compressibility of rocks, *J. Geophys. Res., 70,* 381–389, 1965*a*.
Walsh, J. B., The effect of cracks on the uniaxial compression of rocks, *J. Geophys. Res., 70,* 399–411, 1965*b*.
Walsh, J. B., Attenuation in a partially melted material, *J. Geophys. Res., 73,* 2209–2216, 1968.
Walsh, J. B., New analysis of attenuation in partially melted rock, *J. Geophys. Res., 74,* 4333–4337, 1969.
Whitcomb, J. H., J. D. Garmany, and D. L. Anderson, Earthquake prediction: Variation of seismic velocities before the San Fernando earthquake, *Science, 180,* 632–635, 1973.
Wu, T. T., The effect of inclusion shape on the elastic moduli of a two-phase material, *Int. J. Solids Struct., 2,* 1–8, 1966.

(Received June 20, 1974;
revised September 9, 1974;
accepted September 9, 1974.)